5-Fluorouracil Enhances the Antitumor Activity of the Glutaminase Inhibitor CB-839 against *PIK3CA*-Mutant Colorectal Cancers

Yiqing Zhao[1,2], Xiujing Feng[1,2], Yicheng Chen[1,2], J. Eva Selfridge[1,2,3], Shashank Gorityala[4], Zhanwen Du[1,2], Janet M. Wang[1], Yujun Hao[1,2], Gino Cioffi[5], Ronald A. Conlon[1,2], Jill S. Barnholtz-Sloan[2,5], Joel Saltzman[3,6], Smitha S. Krishnamurthi[3,6], Shaveta Vinayak[3,6], Martina Veigl[2,6], Yan Xu[4], David L. Bajor[2,3,6], Sanford D. Markowitz[2,3,6], Neal J. Meropol[2,3,7], Jennifer R. Eads[2,3,8], and Zhenghe Wang[1,2]

ABSTRACT

PIK3CA encodes the p110α catalytic subunit of PI3K and is frequently mutated in human cancers, including ∼30% of colorectal cancer. Oncogenic mutations in *PIK3CA* render colorectal cancers more dependent on glutamine. Here we report that the glutaminase inhibitor CB-839 preferentially inhibits xenograft growth of *PIK3CA*-mutant, but not wild-type (WT), colorectal cancers. Moreover, the combination of CB-839 and 5-fluorouracil (5-FU) induces *PIK3CA*-mutant tumor regression in xenograft models. CB-839 treatment increased reactive oxygen species and caused nuclear translocation of Nrf2, which in turn upregulated mRNA expression of uridine phosphorylase 1 (UPP1). UPP1 facilitated the conversion of 5-FU to its active compound, thereby enhancing the inhibition of thymidylate synthase. Consistently, knockout of UPP1 abrogated the tumor inhibitory effect of combined CB-839 and 5-FU administration. A phase I clinical trial showed that the combination of CB-839 and capecitabine, a prodrug of 5-FU, was well tolerated at biologically-active doses. Although not designed to test efficacy, an exploratory analysis of the phase I data showed a trend that *PIK3CA*-mutant patients with colorectal cancer might derive greater benefit from this treatment strategy as compared with *PIK3CA* WT patients with colorectal cancer. These results effectively demonstrate that targeting glutamine metabolism may be an effective approach for treating patients with *PIK3CA*-mutant colorectal cancers and warrants further clinical evaluation.

Significance: Preclinical and clinical trial data suggest that the combination of CB-839 with capecitabine could serve as an effective treatment for *PIK3CA*-mutant colorectal cancers.

Introduction

It is well documented that cancer cells *in vitro* can utilize glutamine as an anaplerotic substrate of the tricarboxylic acid (TCA) cycle to generate ATP and precursors for the synthesis of lipids, nucleotides, and other macromolecules to sustain rapid tumor growth (1). Glutamine enters into cells by its transporter Slc1A5 (2). To enter the TCA cycle, glutamine is first converted to glutamate by glutaminases (GLS), then to α-ketoglutarate, a TCA cycle intermediate, by either aminotransferases or glutamate dehydrogenases (2). Our recent study shows that tumors *in vivo* also use glutamine as a fuel source to replenish the TCA cycle (3). In fact, targeting glutamine metabolism has shown promising results in preclinical models in a variety of tumor types including breast, kidney, lung, and pancreatic cancers, as well as acute myeloid leukemia, where all show *in vivo* sensitivity to the glutaminase inhibitor CB-839 (4–12). GLS1 and GLS2 are the two genes encoding glutaminases in human (13). GLS1 is expressed predominantly in kidney and cancers, whereas GLS2 is expressed in liver (13). CB-839 is a potent inhibitor of GLS1 (4).

PIK3CA, which encodes the catalytic subunit of PI3Kα (14, 15), is mutated in a wide variety of human cancers, including ∼30% of colorectal cancers (16, 17). However, an effective approach targeting *PIK3CA* mutations in patients with colorectal cancer is yet to be developed (18). We recently found that PIK3CA mutations render colorectal cancer cells dependent on glutamine (3, 19, 20). This dependency is associated with the upregulation of mitochondrial glutamate pyruvate transaminase 2 (GPT2; ref. 19), which converts glutamate to α-ketoglutarate. Moreover, we demonstrated that aminooxyacetate (AOA), a pan-aminotransferase inhibitor, suppresses xenograft tumor growth of *PIK3CA*-mutant, but not wild-type (WT), colorectal cancer (19).

Here we show that CB-839 preferentially inhibits *PIK3CA*-mutant colorectal cancers. Moreover, CB-839, in combination with 5-fluorouracil (5-FU), induces tumor regression of *PIK3CA*-mutant colorectal cancers in multiple xenograft models. These preclinical data prompted a phase I clinical trial to assess the safety and toxicity profile of a combination of CB-839 and capecitabine (an oral prodrug of 5-FU) in advanced solid tumor patients. Consistent with our preclinical data, an exploratory analysis of the clinical trial data shows a trend that patients with colorectal cancer whose tumors harbor *PIK3CA* mutations may derive a greater clinical benefit from this treatment

[1]Department of Genetics and Genome Sciences, Case Western Reserve University, Cleveland, Ohio. [2]Case Comprehensive Cancer Center, Case Western Reserve University, Cleveland, Ohio. [3]Seidman Cancer Center, University Hospitals Cleveland Medical Center, Cleveland, Ohio. [4]Department of Chemistry, Cleveland State University, Cleveland, Ohio. [5]Department of Population and Quantitative Health Sciences, Case Western Reserve University, Cleveland, Ohio. [6]Department of Medicine, Case Western Reserve University, Cleveland, Ohio. [7]Flatiron Health, New York, New York. [8]Department of Medicine, University of Pennsylvania, Philadelphia, Pennsylvania.

Note: Supplementary data for this article are available at Cancer Research Online (http://cancerres.aacrjournals.org/).

Y. Zhao, X. Feng, and Y. Chen contributed equally to this article.

Corresponding Authors: Zhenghe Wang, Case Western Reserve University, 10900 Euclid Avenue, WRB 3120, Cleveland, OH 44106. Phone: 216-368-0446; Fax: 216-368-8919; E-mail: zxw22@case.edu; and Jennifer R. Eads, Jennifer.Eads@pennmedicine.upenn.edu

Cancer Res 2020;80:4815–27

doi: 10.1158/0008-5472.CAN-20-0600

strategy as compared with those with *PIK3CA*-WT tumors. Together, the data suggest that targeting glutamine metabolism may be an effective approach for treating patients with *PIK3CA*-mutant colorectal cancer.

Materials and Methods

Cell culture and chemicals

Colorectal cancer cell lines, HCT116, DLD1, RKO, and SW480 were obtained from ATCC. These cell lines were cultured in McCoy's 5A medium containing 10% FBS, as described previously (21). The tissue culture cell lines are routinely checked for mycoplasma contamination. The cell lines were authenticated by the Genetica DNA Laboratories using STR profiling. CB-839 was kindly provided by Calithera Biosciences. Oxaliplatin, camptothecin, and regorafenib were purchased from Selleck Chemical. 5-Fluorouracil was purchased from Sigma-Aldrich.

Drug treatment of xenograft tumors

Animal experiments were approved by the Case Western Reserve University Animal Care and Use Committee and performed in accordance with relevant guidelines and regulations.

Subcutaneous xenografts were established as described in ref. 22. Three million cells were injected subcutaneously into the flanks of 6- to 8-week-old female athymic nude mice. When tumors reached around 250 to 400 mm^3, mice were randomly divided into groups (10 tumors for each group). Mice were treated with CB-839 (200 mg/kg) once or twice daily by oral gavage, 5-FU (30 mg/kg) once a day by intraperitoneal injection, or both CB-839 and 5-FU. Tumor volume was measured with electronic calipers, and volumes were calculated by the formula of length $\times$ width^2/2. For patient-derived xenograft (PDX) models, tumors were first sliced into approximately 4 mm^3 pieces and implanted subcutaneously into nude mice. When the average tumor volume reached around 250 to 400 mm^3, mice were treated with the indicated drugs, and tumors were measured once per week.

Flow cytometry

Cells were plated in six-well plates at 2×10^5 cells per well in complete medium. After 24 hours, drugs were added into the medium. Cells were treated by the drugs for 24 hours and then collected by trypsinization. Cells were fixed in 70% ethanol overnight at 4°C and stained with propidium iodide before flow cytometry analyses as described previously (23). Sub-G_1 phase cells were classified as cell death.

Immunoblotting

Cells were plated into six-well plates. Sixteen hours later, the indicated drugs or compounds were added into the medium. After 24 hours, cells were lysed with RIPA buffer [10 mmol/L Tris (pH 7.4), 150 mmol/L NaCl, 5 mmol/L EDTA, 0.1% SDS, 1% Triton-X100, 1 mmol/L DTT, 1 mmol/L PMSF, complete Protease Inhibitor Cocktail tablet (Roche)]. Then lysates were cleared by centrifugation (14,000 rpm, 10 minutes) and protein concentration was determined by the BCA Protein Assay Kit (Pierce). Equal amounts of total protein were used for immunoblotting as described previously (24). The following antibodies were used: Cell Signaling Technology: rabbit polyclonal anti-cleaved PARP (catalog no. 9544), rabbit McAb xCT/SLC7A11(catalog no. 12691), mouse McAb NQ01(catalog no. 3187); Novus Biologicals: Mrp5 (catalog no. NBP2–46467), and Mrp8 (catalog no. NBP1–59810); Sigma-Aldrich: mouse monoclonal Anti-β-Actin (catalog no. A5441); Santa Cruz Biotechnology: Nrf2, Lamin B2, and GAPDH.

Microarray

HCT116 and DLD1 *PIK3CA* WT or Mut cells were grown with or without glutamine for 24 hours. RNAs were extracted for microarray analyses. Input RNA was provided at 50 ng/μL and the labeling reaction was initiated with 150 ng of RNA samples for interrogation on the expression microarrays following the manufacturer's instructions. Samples were labeled robotically using the Affymetrix WT (whole transcript) labeling protocol and the Beckman Coulter Biomek FX^P Laboratory Automation Workstation; scripts were provided by Affymetrix to process up to 96 samples in batch. Samples were interrogated on the Human Gene Array 2.1 in the PEG format. Hybridization, washing, staining and data collection were carried out in the Affymetrix Gene Titan MC (multichannel) instrument. The Microarray data were deposited into GEO (accession no. GSE157024).

Reverse transcription PCR

RNAs were extracted using either RNeasy Plus Mini Kits (Qiagen) according to the manufacturer's instructions. One microgram of each total RNA was used for reverse transcription using the Superscript III First-Strand Synthesis Kit (Thermo Fisher Scientific). The resulting cDNAs were diluted 5-fold with double-distilled water and were used as templates for reverse transcription PCR (RT-PCR). Primers used are listed below: for uridine phosphorylase 1 (UPP1) expression: forward: 5′-AACAGAGCAGGCAGTGGATA-3′; reverse: 5′-ATACGCCTGCTTGTCCTTCT-3′. For GAPDH: forward: 5′-GGAAATCCCATCACCATCT-3′; reverse: 5′-TGTCGCTGTTGAAGTCAGA-3′

Real-time-RT PCR

RNAs were extracted using either RNeasy Plus Mini Kits (Qiagen) for cells or TRIzol (Thermo Fisher Scientific) for tumor samples according to the manufacturer's instructions. The Taqman assay system was used for qRT-PCR using UPP1 probes (Hs00370287; Applied Biosystems) with IQ super mix (catalog no. 170-8860; Bio-Rad). Expression levels of UPP1 in each sample was normalized to that of β2-microglobulin.

Reactive oxygen species and glutathione measurement

Reactive oxygen species (ROS) was measured by labeling cells with H2-carboxy-DCFDA (Invitrogen) according to the manufacturer's instructions. GSH/GSSG ratios were measured with a GSH/GSSG Ratio Assay Kit (Bio Vision) according to the manufacturer's instructions.

Nuclear fractionation

Cells were treated with the given chemicals overnight at the indicated concentrations. By the end of the treatment, cells were washed with ice-cold PBS once and then lysed in harvest buffer (10 mmol/L HEPES pH 7.9, 50 mmol/L NaCl, 0.5M sucrose, 0.1 mmol/L EDTA, 0.5% Triton X-100, and freshly added 1 mmol/L DTT). Cell lysates were incubated on ice for 5 minutes and nuclei were harvested by centrifuging at 500 $\times$ *g* for 5 minutes at 4°C. The supernatants were transferred to new tubes and spun down at 14,000 $\times$ *g* for 10 minutes. Nuclear pellets were washed twice with buffer A (10 mmol/L HEPES pH 7.9, 10 mmol/L KCl, 0.1 mmol/L EDTA, 0.1 mmol/L EGTA, and freshly added 1 mmol/L DTT), and lysed in buffer C (10 mmol/L HEPES pH 7.9, 500 mmol/L NaCl, 0.1 mmol/L EDTA, 0.1 mmol/L EGTA, 0.1% NP-40, and freshly added 1 mmol/L DTT) for 10 minutes on ice. The nuclear lysates were centrifuged at the highest speed for 10 minutes and supernatants were taken as nuclear fractions.

siRNA knockdown

Two independent siRNA against Nrf2 were purchased from IDT (reference nos. hs.Ri.NFE2L2.13.1 and hs.Ri.NFE2L2.13.3). The siRNAs were transfected into HCT116 cells using Lipofectamine 2000 according to the manufacturer's instructions.

Chromatin immunoprecipitation

Chromatin immunoprecipitation (ChIP) assays were performed using a SimpleChIP Enzymatic Chromatin IP Kit (Cell Signaling Technologies; catalog no. 9003) and as described previously (25). Briefly, cells were cross-linked with 37% formaldehyde at a final concentration of 1% at room temperature for 10 minutes. Fragmented chromatin was treated with nuclease and subjected to sonication. ChIP was performed with an anti-NRF2 antibody (Cell Signaling Technologies, catalog no. 12721) or normal rabbit IgG (Cell Signaling Technologies, catalog no. 2729). After DNA purification, immunoprecipitated DNA was quantified by real-time PCR using iQ SYBR Green Supermix (Bio-Rad, catalog no. 1708880) with primers for UPP1 promoter (Forward: CTGGAGCATTGCGTTTGTC; Reverse: GACCCCTGGGAAGAGAGAAC); HMOX1 promoter (Cell Signaling Technologies, catalog no. 53538) and RPL30 exon 3 (Cell Signaling Technologies, catalog no. 7014). Fold enrichment was calculated on the basis of the threshold cycle (CT) value of the IgG control using the comparative CT method.

Cellular thermal shift assay

The cellular thermal shift assay (CETSA) was performed as described (26). Briefly, for tissue culture cells, cells were plated in six-well plates at 2×10^5 per well. When the cells reached ∼70% confluence, they were treated with DMSO or CB-839 (5 μmol/L) overnight, and then treated with DMSO or 5-FU (1 μmol/L) for 2 hours. Cells were harvested, washed with PBS, and resuspended in PBS supplemented with protease/phosphatase inhibitors. The cell suspension was heated at 52°C for 3 minutes in a thermal cycler followed by cooling for 3 minutes at room temperature. For Western blot analyses, the cells were lysed in kinase buffer [25 mmol/L Tris-HCl (pH 7.5), 5 mmol/L β-glycerophosphate, 2 mmol/L DTT, 0.1 mmol/L Na_3VO_4, 10 mmol/L $MgCl_2$] by using three cycles of freeze–thaw. The lysates were centrifuged at 20,000 × *g* for 20 minutes at 4°C to remove the precipitates. The supernatants were analyzed by Western blot analysis using a rabbit anti-TS antibody (Proteintech, catalog no. 15047-1-AP). For AlphaLISA assay, cells were lysed in CETSA Cell Lysis Buffer 2 (Perkin Elmer, catalog no. CETSA-BUF2-100ML) and AlphaLISA was performed according to the manufacturer's instructions (Perkin Elmer). A mouse (Santa Cruz Biotechnology, catalog no. sc-376161) and the rabbit anti-TS antibodies were used for the AlphaLISA.

For tumor tissues, frozen tumor tissues were homogenized in cold PBS containing protease/phosphatase inhibitors using tissue grinders followed by three cycles of freeze–thaw. The lysate was separated from the cell debris by centrifugation at 20,000 × *g* for 20 minutes at 4°C. The tissue lysates were heated at 48°C for AlphaLISA.

Immunofluorescence

Immunofluorescent staining was performed as described previously (27). Briefly, cells were fixed with 4% paraformaldehyde for 15 minutes at room temperature in a multiwell plate. The plate was incubated with blocking buffer (1× PBS, 5% normal serum, and 0.3% Triton X-100) for 1 hour and then incubated overnight with phosphohistone H2A.X antibody (Cell Signaling Technology, catalog no. 80312) in antibody dilution buffer (1× PBS, 1% BSA, and 0.3% Triton X-100) at 4°C. After being washed three times with PBS, the cells were incubated with a secondary Alexa Fluor 488-conjugated antibody. The nuclei were labeled with 4′,6-diamidino-2-phenylindole (DAPI; Sigma, catalog no. D9542).

UPP1 knockout

UPP1 knockout clones were generated using the CRISPR/Cas9 system. Two different guide RNAs were used to target the UPP1 gene. sgRNA 1 (5′-TGCCTCAGTTGGCGGAATGG) targets exon 3 of UPP1 genomic sequence and sgRNA2 (5′-TCAGGGCAAGGCCGTCTGGA) targets exon 8. A targeting plasmid expressing sgRNA1 or sgRNA2 and CAS9 protein was transfected into HCT116 cells. Single clones were picked up to screen for targeted clones by genomic PCR. Knockout clones were verified by sequencing both genomic DNA and RNA.

dTTP measurement

Cell pellets (approximately 10 million cells) frozen at −70°C were thawed at room temperature for 15 minutes. Then 500 μL of 80% methanol–water was added and vortexed for 5 minutes to resuspend the pellet, followed by incubation at −70°C for 30 minutes. This was repeated two times, and finally, the suspension was sonicated for 10 minutes to completely break the cells and release their contents. The suspension was centrifuged at 13,000 × *g* for 10 minutes. The supernatant was separated and dried using N2 at 35°C for 20 minutes. Finally, the residue was reconstituted in 100 μL water and subjected to LC/MS-MS analysis. For LC/MS-MS analysis, 2′-deoxyadenosine-13C10,15N5 5′-triphosphate (Sigma-Aldrich) was used as internal standard. The separation of analytes was achieved by a Shimadzu LC-20AD HPLC system with a Shimadzu SIL-20AC autosampler (Shimadzu) on a YMC-ODS-AM column (2.1 × 100 mm, 3.0 μm) using gradient mode of elution with mobile phase A: 5 mmol/L N,N-dimethyl hexylamine in water, 10 mmol/L ammonium bicarbonate, and B: 50:50 acetonitrile:water, 5 mmol/L N,N-dimethyl hexylamine, 10 mmol/L ammonium bicarbonate at a flow rate of 0.200 mL/min. The column was eluted by 10% B mobile phase for 1 minute, then from 10% to 25% B for 4 minutes, 25% B for 15 minutes, from 25% to 55% B for 1 minute, 55% B for 7 minutes, from 55% to 10% B for 1 minute, and then 10% B for 9 minutes. Quantitation of the analytes was accomplished by an AB Sciex API 3200 triple quadruple tandem mass spectrometer (AB Sciex), which was operated in the negative multiple-reaction-monitoring mode with mass transition 481.1 > 159.0 for dTTP.

Phase I clinical trial design

This clinical trial was conducted with the approval of the institutional review board and according to good clinical practice with a primary objective of determining the MTD and dose-limiting toxicities (DLT) of oral CB-839 (provided by Calithera Biosciences) when administered with oral capecitabine. Dosing was based on a standard 3+3 dose escalation schedule. Response to therapy was assessed per RECIST 1.1 utilizing CT imaging obtained every 9 weeks. Patients were permitted to continue treatment until disease progression or development of unacceptable toxicity (Supplementary Fig. S6A). All patients provided written informed consent prior to participating in the study. The trial was registered in clinicaltrials.gov (NCT02861300).

Eligibility

Patients were eligible for study entry if they had an advanced solid tumor and had progressed on all standard lines of therapy, or if capecitabine was an appropriate treatment option for them. Patients with colorectal cancer specifically must have progressed on prior

fluoropyrimidine-based chemotherapy. Patients otherwise must have been at least 18 years of age, had an ECOG performance status of 0 or 1, had normal bone marrow, renal, and hepatic function, had the ability to swallow pills and be able to understand and the willingness to sign consent. Patients were not eligible if they had ongoing treatment-related toxicities that were greater than grade 1 and they could not be receiving other investigational agents. Central nervous system involvement by their cancer or prior allergic reaction to either CB-839 or capecitabine was not permitted.

Dose-limiting toxicities

Toxicity was assessed utilizing the Common Terminology Criteria for Adverse Events (CTCAE) version 4.0. To be evaluable for a DLT, patients must have received at least 75% of the planned CB-839 and capecitabine during the first treatment cycle (21 days). A DLT was defined as any ≥ grade 3 nonhematologic toxicity thought to be treatment-related, grade 3 febrile neutropenia, ≥ grade 3 thrombocytopenia associated with ≥ grade 3 bleeding, grade 4 neutropenia or grade 4 thrombocytopenia occurring during the 21-day DLT window. At dose level four, one patient was replaced for not receiving enough study drug to be evaluable.

Statistical analysis

GraphPad Prism software was used to create the graphs. Data are plotted as mean ± SEM. We applied the *t* test to compare the means between two groups, assuming unequal variances. For xenograft growth, we carried out ANOVA for repeated measurements to test whether there is an overall difference in the tumor sizes by testing group differences as well as whether there was a difference in the development of tumor sizes over time between the two groups by testing the interaction between time and group. Kaplan–Meier analysis was used to assess differences in progression-free survival (PFS) stratified by *PI3KCA* mutation status for patients with colorectal cancer only, generating a log-rank *P* value as well as median survival time with 95% confidence intervals (95% CI). Patient response to therapy during the phase I clinical trial was defined per RECIST criteria. Patients were considered evaluable for response if they had measurable disease at the time of study entry, had received at least one cycle of therapy and had undergone a repeat disease evaluation with imaging. PFS was defined as the time from the beginning of treatment to RECIST evidence of progressive disease as determined by radiography or by clinical progression.

Results

CB-839 inhibits growth of *PIK3CA*-mutant, but not WT, colorectal cancers

We have showed previously that *PIK3CA* mutations render colorectal cancers dependent on glutamine (19) and that CB-839 targets glutaminase in cultured colorectal cancer cells and xenograft tumors (28). Thus, we set out to determine the sensitivity of the isogenic *PIK3CA* mutant-only (Mut, with the WT allele being knocked out) and WT-only (WT, with the mutant allele being knocked out) colorectal cancer cell line pairs to CB-839 (Supplementary Fig. S1A). As shown in Supplementary Figs. S1B and S1C, HCT116 and DLD1 *PIK3CA* Mut cell lines are more sensitive to CB-839 than the corresponding isogenic *PIK3CA* WT cell lines. Consistent with our previous observation that *KRAS* mutations have no impact on glutamine dependency of colorectal cancer cells (19), isogenic HCT116 *KRAS* WT and mutant cell lines had similar sensitivity to CB-839 (Supplementary Figs. S1D and S1E). We next tested if CB-839 preferentially suppresses xenograft tumor growth of *PIK3CA*-mutant cells. As shown in **Fig. 1A**, CB-839 significantly inhibited xenograft tumor growth of HCT116 cells, which harbor a *PIK3CA* mutation, regardless of once or twice daily drug exposure. Moreover, CB-839 treatment also significantly inhibited tumor growth of a colon cancer PDX harboring a *PIK3CA* mutation (**Fig. 1B**). In contrast, CB-839 had no effect on *PIK3CA*-WT xenograft tumors established from SW480 colorectal cancer cells or a *PIK3CA*-WT colorectal cancer PDX model (**Fig. 1C** and **D**). Taken together, our data demonstrate that CB-839 preferentially inhibits the growth of *PIK3CA*-mutant, but not WT, colorectal cancers.

Combination of CB-839 with 5-FU promotes regression of *PIK3CA*-mutant colorectal cancer xenografts

In an attempt to identify clinically useful drugs that might enhance the tumor inhibitory effect of CB-839 against colorectal cancer, we tested combinations of CB-839 with 5-FU, camptothecin, oxaliplatin, and regorafenib in HCT116 cells. As shown in **Fig. 2A** and Supplementary Fig. S2A, an additive effect on apoptosis, was only observed when CB-839 was combined with 5-FU.

We then went on to test whether 5-FU enhances the efficacy of CB-839 on *PIK3CA*-mutant colorectal cancers in subcutaneous xenograft models. As shown in **Fig. 2B** to **D**, the combination of CB-839 and 5-FU induced regression of xenograft tumors established from HCT116 and RKO (another *PIK3CA*-mutant colorectal cancer cell line). Although CB-839 or 5-FU alone inhibited tumor growth to various extents, neither induced tumor regression (**Fig. 2C** and **D**). Moreover, the CB-839 plus 5-FU combination induced tumor regression of a *PIK3CA*-mutant colon cancer PDX that was derived from a metastatic liver lesion of a patient (**Fig. 2E**). Notably, a third of the initial tumor lesions in each of these xenograft models appeared to be completely eliminated by the drug combination and no evidence of tumor regrowth was seen in these mice one month after the treatment was stopped. Finally, although the drug combination did not induce regression of DLD1 xenograft tumors (also harboring a *PIK3CA* mutation), it potently inhibited the progressive growth of these tumors (**Fig. 2F**). To further ascertain that the drug combination preferentially induced tumor regression in *PIK3CA*-mutant tumors, we treated xenograft tumors established from the isogenic HCT116 *PIK3CA* Mut and WT cell lines. As shown in Supplementary Fig. S2B, the CB-839 and 5-FU combination induced regression of the HCT116 *PIK3CA*-mutant, but not the *PIK3CA* WT, tumors. Together, the data suggest the combination of CB-839 and 5-FU might be an effective treatment for *PIK3CA*-mutant colorectal cancers.

CB-839 treatment upregulates gene expression of uridine phosphorylase 1

To determine the mechanism by which CB-839 enhances the tumor inhibitory effect of 5-FU in *PIK3CA*-mutant colorectal cancers, we profiled gene expression of the isogenic *PIK3CA* Mut and WT colorectal cancer cell lines. Given that CB-839 blocks glutamine utilization and that it mirrors glutamine deprivation, we performed microarray analyses of HCT116 and DLD1 *PIK3CA* Mut and WT cell lines cultured without glutamine for 24 hours. **Figure 3A** shows the volcano plots of gene expression changes in *PIK3CA* Mut cells versus WT cells. Gene ontology (GO) pathway analysis showed that genes involved in chromosome structure, cell cycle, DNA damage repair, thymidine metabolism, and others were enriched (Supplementary Fig. S3A). Interestingly, only 12 genes, including *UPP1*, were commonly upregulated in both HCT116 and DLD1 *PIK3CA*-mutant cell lines (Supplementary Fig. S3B). We turned our

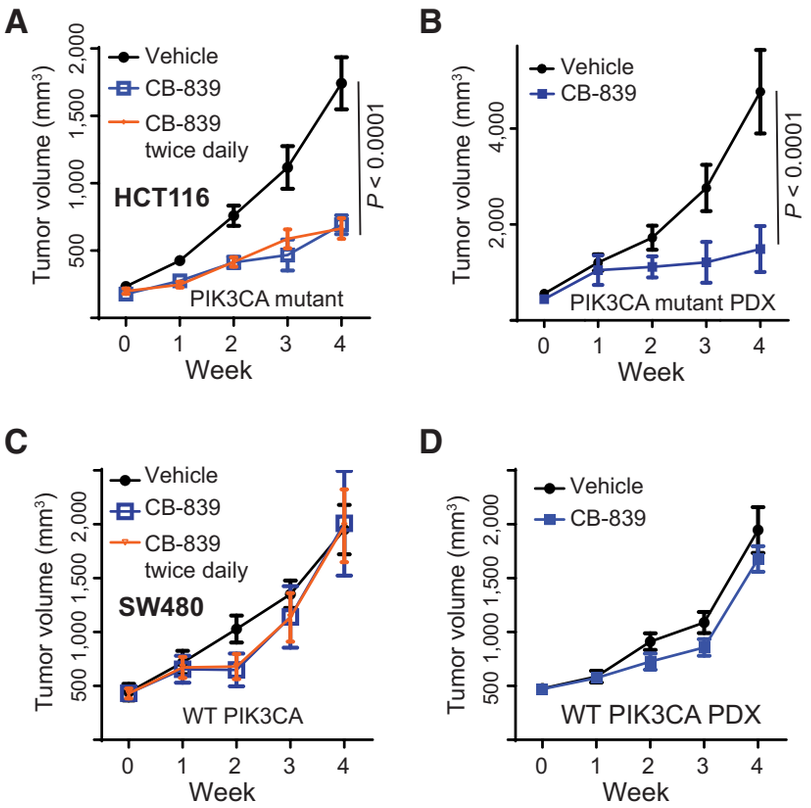

Figure 1.

CB-839 inhibits xenograft tumor growth of *PIK3CA*-mutant, but not WT, colorectal cancers. Subcutaneous xenograft tumors established from the indicated cell line or PDX. Once tumors reached 200 to 400 mm^3, mice (5 mice with 10 tumors in each group) were treated with vehicle, CB-839 (200 mg/kg), once or twice per day orally. **A,** HCT116. **B,** A *PIK3CA*-mutant colon cancer PDX. **C,** SW480. **D,** A WT *PIK3CA* colon cancer PDX. ANOVA was used for statistical analyses.

attention to *UPP1* gene for the following reasons: (i) *UPP1* gene expression is ranked as the second-highest upregulated gene in both HCT116 and DLD1 *PIK3CA* Mut cells versus PIK3CA WT cells; (ii) UPP1 facilitates the conversion of 5-FU to FdUTP (29); and (iii) *PIK3CA*$^{-/-}$ ES cells are 10-fold more resistant to 5-FU (30). qRT-PCR analyses showed that both glutamine deprivation and CB-839 treatment-induced highest level UPP1 in *PIK3CA* Mut cell lines (**Fig. 3B** and **C**), although *PIK3CA* Mut cell lines had higher basal levels of UPP1 than their WT counterparts (**Fig. 3C**). Moreover, CB-839 treatment also induced *UPP1* gene expression in HCT116 xenograft tumors (**Fig. 3D**). It is worth noting that there is no difference in *UPP1* mRNA levels between colorectal cancers and normal colon tissues (Supplementary Fig. S3C).

CB-839 treatment induces high levels of ROS in *PIK3CA*-mutant cells, Nrf2 nuclear translocation, and increased UPP1 gene expression

To interrogate how CB-839 treatment induces UPP1expression in PIK3CA-mutant cells, we turned our attention to Nrf2 for the following reasons: (i) UPP1 was shown to be a transcriptional target of Nrf2 (31); (ii) Nrf2 is a latent transcription factor that is activated by oxidative stress through protein stabilization and nuclear translocation (32); and (iii) glutamine starvation increases ROS (33). Thus, we postulated that CB-839 treatment might increase ROS levels, which in turn activate Nrf2 and increase UPP1 transcription. Indeed, CB-839 treatment significantly increased ROS levels in *PIK3CA* WT and Mut cells derived from both HCT116 and DLD1 (**Fig. 4A**), although the *PIK3CA* Mut cells had higher basal levels of ROS than *PIK3CA* WT cells (**Fig. 4A**). Consistently, CB-839 treatment reduced the ratio of reduced versus oxidized forms of glutathione in the HCT116 and DLD1 cell lines (**Fig. 4B**). As expected, CB839 treatment increased the levels of nuclear Nrf2 in the HCT116 and DLD1 *PIK3CA* WT and *PIK3CA* Mut cell lines, but the nuclear levels of Nrf2 are higher in the *PIK3CA* Mut cell lines treated with CB-839 than in the *PIK3CA* WT cell lines (**Fig. 4C**). Consistent with a report that the PI3K–AKT pathway regulates Nrf2 nuclear translocation (34), Supplementary Fig. S4A shows that nuclear Nrf2 levels were markedly decreased in p110α lipid kinase-dead DLD1 mutant cells that we generated previously (19). To validate that Nrf2 modulates *UPP1* gene expression, we knocked down Nrf2 with two independent siRNAs. As shown in **Fig. 4D**, knockdown of Nrf2 reduced CB-839-induced *UPP1* gene expression, although knockdown of Nrf2 also decreased basal levels of UPP1 (**Fig. 4D**). Conversely, overexpression of Nrf2 increased UPP1 expression (**Fig. 4E**). Moreover, ChIP-qPCR analyses demonstrated that Nrf2 bound to a promoter region of *UPP1* (**Fig. 4F**). Although *NRF2* mutations are rare in colorectal cancers, an analysis of the pan-cancer The Cancer Genome Atlas data showed that *NRF2* mutant colorectal cancers expressed significantly higher levels of UPP1 than NRF2 WT colorectal cancers (**Fig. 4G**). Taken together, these data suggest that CB-839 treatment induces higher levels of ROS in *PIK3CA* mutant cells, which in turn increases nuclear Nrf2 levels and thus upregulates UPP1 mRNA expression.

It has been reported that the cystine/glutamate antiporter xCT/SLC7A11, an Nrf2 transcriptional target (35), drives glutamine dependency in lung cancer (36). We thus examined protein levels of SLC7A11 and other Nrf2 targets in the isogenic HCT116 and DLD1 *PIK3CA* Mut and WT cell line pairs. SLC7A11 protein levels were not upregulated in the *PIK3CA* Mut cell lines compared with its isogenic WT counterparts (Supplementary Fig. S4B). Moreover, an xCT inhibitor, sulfasalazine, did not suppress the growth of HCT116 colorectal

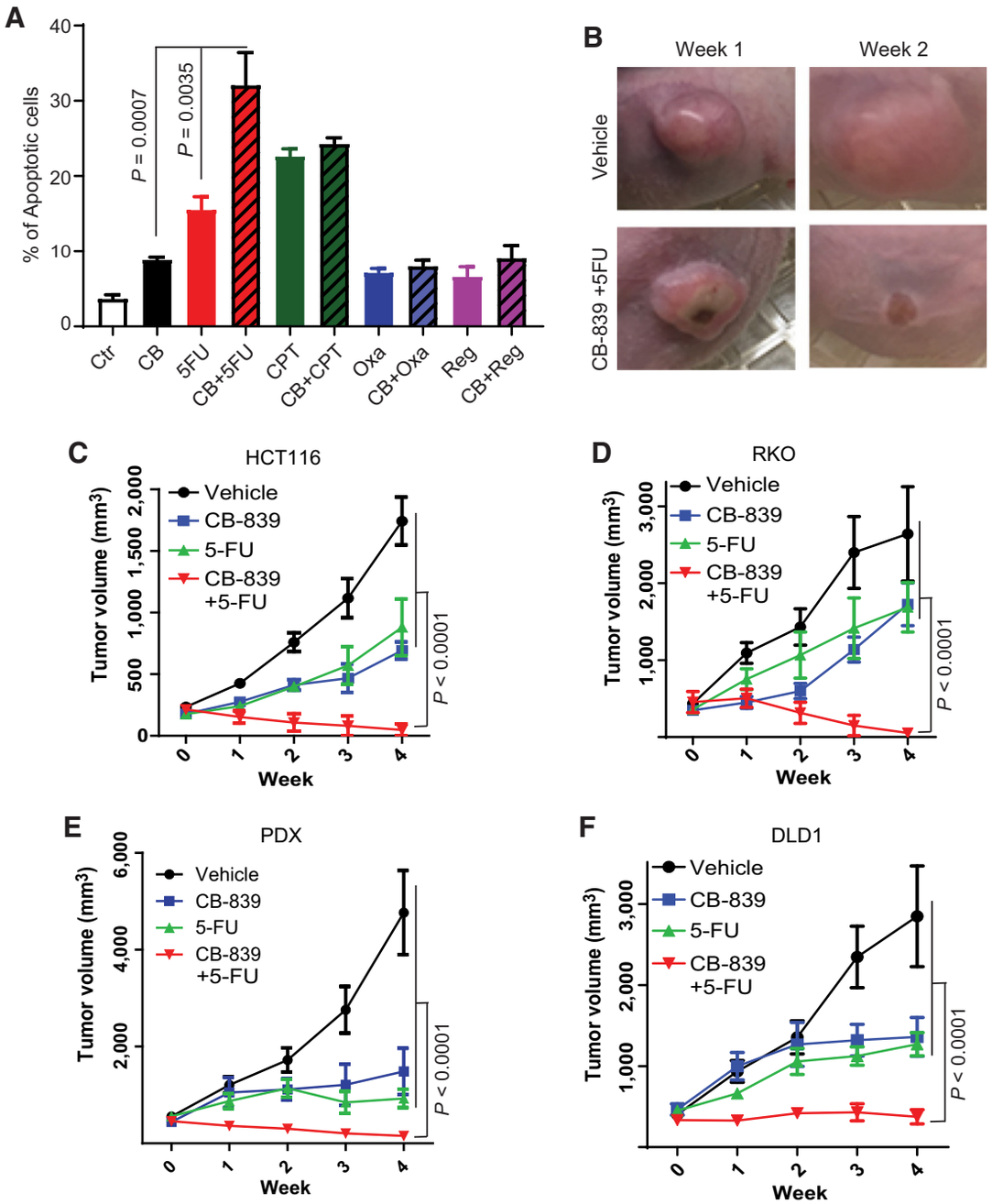

Figure 2.

CB-839 combined with 5-FU shrinks *PIK3CA*-mutant colorectal cancers *in vivo*. **A,** Induction of apoptosis by colon cancer drugs alone and in combination with CB-839. HCT116 cells were treated with the indicated drugs for 24 hours [CB-839 (20 μmol/L); 5-FU (10 μmol/L); camptothecin (CPT, 25 nmol/L); oxaliplatin (Oxa, 25 μmol/L); regorafenib (Reg, 25 μmol/L)]. Percentages of apoptotic cells are plotted. **B–F,** When the indicated xenograft tumors reached ∼200 to 400 mm^3 in size, mice were treated daily with vehicle, CB-839 (200 mg/kg, oral gavage), 5-FU (30 mg/kg, i.p.), or CB-839 with 5-FU (5 mice/group). Representative images of an HCT116 tumor regressing over time in the combination treatment group (**B**). Growth curves of tumors established from HCT116 are shown in **C**, RKO in **D**, a *PIK3CA*-mutant colon cancer PDX in **E**, and DLD1 in **F**. ANOVA was used for statistical analyses.

cancer cells (Supplementary Fig. S4C) even at 100 μmol/L concentration. In contrast, CB-839 markedly inhibited HCT116 cell growth at low μmol/L concentrations (Supplementary Fig. S4C). The data suggest that differential sensitivity of *PIK3CA*-mutant versus WT colorectal cancers to CB-839 is not due to the cystine/glutamate antiporter xCT/SLC7A11.

Multidrug resistance-associated protein (Mrp) transporters, including Mrp3 and Mrp4, are reported as the transcriptional targets of

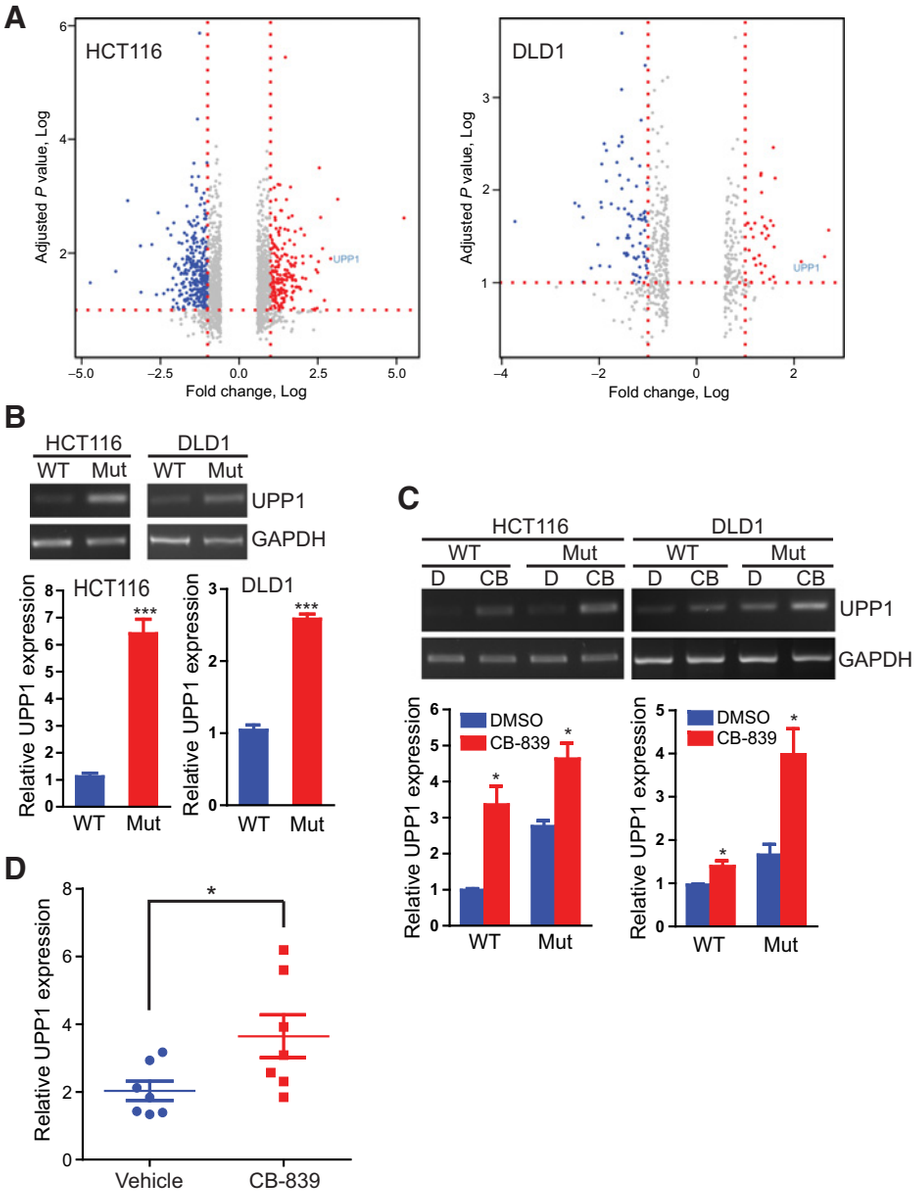

Figure 3.

CB-839 treatment induces gene expression of UPP1. **A,** Microarray analysis of isogenic *PIK3CA*-mutant and WT HCT116 and DLD1 cell lines cultured in the absence of glutamine. Fold changes of gene expression in *PIK3CA* Mut cells versus in the corresponding WT cells are plotted as volcano plots. **B,** qRT-PCR analyses of UPP1 expression in the indicated cell lines deprived of glutamine. **C,** qRT-PCR analyses of UPP1 expression in the indicated cell lines treated with CB-839 (CB) or DMSO (D). **D,** qRT-PCR analyses of UPP1 expression in xenograft tumors treated with either vehicle or CB-839. *, $P < 0.05$; ***, $P < 0.001$; *t* test.

Nrf2 (37), whereas an upregulation of Mrp5 or Mrp8 is known to cause 5-FU resistance in cancer cells (38, 39). We thus set out to determine if CB-839 treatment caused changes in Mrp5 and Mrp8, thereby modulating 5-FU sensitivity. As shown in Supplementary Fig. S4D, CB-839 treatment had no impact on Mrp5 and Mrp8 protein levels. The data suggest CB-839 treatment is unlikely to affect the export of 5-FU or its metabolites.

CB-839 enhances the binding of 5-FU metabolite to thymidylate synthetase

UPP1 catalyzes the reversible phospholytic cleavage of uridine and deoxyuridine to uracil and ribose- or deoxyribose-1-phosphate, thereby facilitating the conversion of 5-FU to FdUMP (29). We thus used a cellular thermal shift assay (40) to test if CB-839 treatment enhanced engagement of FdUMP with its target thymidylate synthase (TS), a major mechanism of 5-FU cytotoxicity (41). As shown in **Fig. 5A** and **B**, CB-839 treatment significantly increased the binding of TS to FdUMP in HCT116 cells in culture. Moreover, CB-839 treatment dramatically increased the binding of TS to FdUMP in xenograft tumors established from both HCT116 and DLD1 cells (**Fig. 5C–F**). Given that TS converts dUMP to dTMP to produce cellular dTTP, we set out to determine how the combination of CB-839 and 5-FU impacts cellular dTTP levels. As shown in **Fig. 5G**, either drug alone significantly reduced amounts of dTTP. However, the combination of CB-839 and 5-FU resulted in near-complete depletion of cellular dTTP (**Fig. 5G**). Because depletion of cellular dTTP can cause DNA damage (42), we determined if the combination of CB-839 and 5-FU induced more DNA damages than the single drug alone by staining drug-treated cells with an anti-p-H2A.X antibody. As shown in **Fig. 5H** and Supplementary Fig. S5A, the combination of CB-839 and 5-FU induced significantly more p-H2A.X positive cells than the single drug alone. Given that incorporation of 5-FU into DNA and

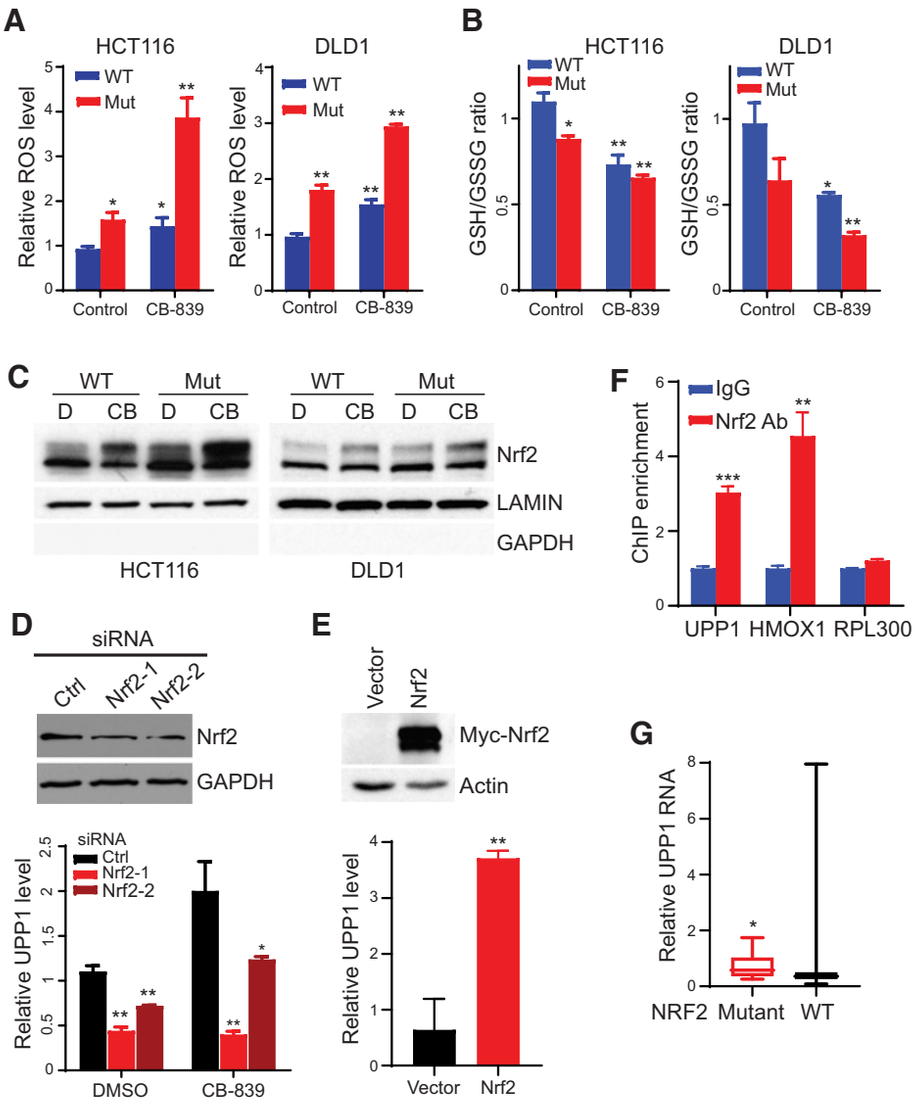

Figure 4.

CB-839 treatment increases cellular ROS levels and induces nuclear Nrf2 translocation, which in turn activates UPP1 mRNA expression. **A** and **B,** The indicated cell lines were treated with either DMSO or CB-839 for 6 hours. Levels of cellular ROS (**A**) and glutathione (**B**) were measured. *, $P < 0.05$; **, $P < 0.01$; *t*-test; columns are compared with the corresponding *PIK3CA* WT cell without CB-839 treatment. **C,** The indicated cells were treated with DMSO or CB-839. Cells were fractionated, and the nuclear fractions were blotted with the indicated antibodies. **D,** The knockdown of Nrf2 reduces UPP1 gene expression. HCT116 cells were transfected with the indicated siRNA and treated with either DMSO or CB-839. Cell lysates were blotted with the indicated antibodies. qRT-PCR was performed to measure UPP1 levels. *, $P < 0.05$; **, $P < 0.01$; *t* test; columns are compared with the corresponding control siRNA. **E,** Overexpression of Nrf2 increases *UPP1* gene expression. HCT116 cells were transfected with a Myc-tagged Nrf2 expression construct. UPP1 expression levels were measured. **, $P < 0.01$; *t* test. **F,** Nrf2 binds to the UPP1 promoter. HCT116 cells were treated with CB-839. ChIP-PCRs were performed with the indicated genes. HMOX1, a known Nrf2 target, served as a positive control. RPL300 served as a negative control. **, $P < 0.01$; ***, $P < 0.001$; *t* test. **G,** NRF2-mutant colorectal cancers express higher levels of UPP1 mRNA than NRF2 WT colorectal cancers. The mRNA expression levels of UPP1 (RNA-seq data in The Cancer Genome Atlas PanCancer Atlas dataset) are plotted into NRF2 mutant ($n = 8$) and WT ($n = 516$) colorectal cancer groups. *, $P < 0.05$; Mann–Whitney test.

RNA is a potential mechanism for the tumor inhibitory effect of 5-FU, we set out to determine if CB-839 treatment increased 5-FU incorporation into DNA and RNA. As shown in Supplementary Fig. S5B, CB-839 treatment actually decreased 5-FU incorporation into DNA and had no impact on 5-FU incorporation into RNA (Supplementary Fig. S5C), thereby ruling out those as the mechanisms by which CB-839 enhances 5-FU activity. Although we attempted to determine if the combination of CB-839 and 5-FU depletes dTTP levels in xenograft tumors, technical limitations of our mass spectrometry method did not allow this analysis on tumor samples. Together, these data suggest that CB-839 treatment increases ROS level, induces nuclear translocation of Nrf2, and upregulates *UPP1* gene expression. This in turn facilitates the conversion of 5-FU to FdUMP and enhances inhibition of TS, thereby leading to depletion of cellular dTTP (**Fig. 5I**).

The knockout of UPP1 abrogates the tumor inhibitory effect of combined CB-839 and 5-FU

To test whether UPP1 plays a critical role in the enhancement of 5-FU activity by CB-839, we set out to knockout (KO) *UPP1* in HCT116 cells with CRISPR/Cas9 genome editing technology by two different strategies (**Fig. 6A**): (i) targeting the starting ATG codon in exon 3 and (ii) targeting the substrate-binding site (amino acids Q217 and R219) encoded by exon 8. Although the two *UPP1* KO cell lines grew as well as the parental cells in tissue culture, they grew significantly slower as xenograft tumors (**Fig. 6B**). Importantly, both *UPP1* knockouts abolished the additive tumor inhibitory effect of CB-839 and 5-FU (**Fig. 6C**). Surprisingly, the *UPP1* KO cell lines were also insensitive to CB-839 treatment alone (**Fig. 6C**). Taken together, our data suggest that the upregulation of UPP1 by CB-839 treatment plays a key role in enhancing the tumor inhibitory effect of 5-FU.

Clinical experience of CB-839 and capecitabine in humans

On the basis of our preclinical data, we conducted a phase I clinical trial to assess the safety and toxicity profile of CB-839 and capecitabine in humans. Specifically, the objective of the study was to determine the MTD and any DLTs of the combination of CB-839 and capecitabine in patients with advanced solid tumors.

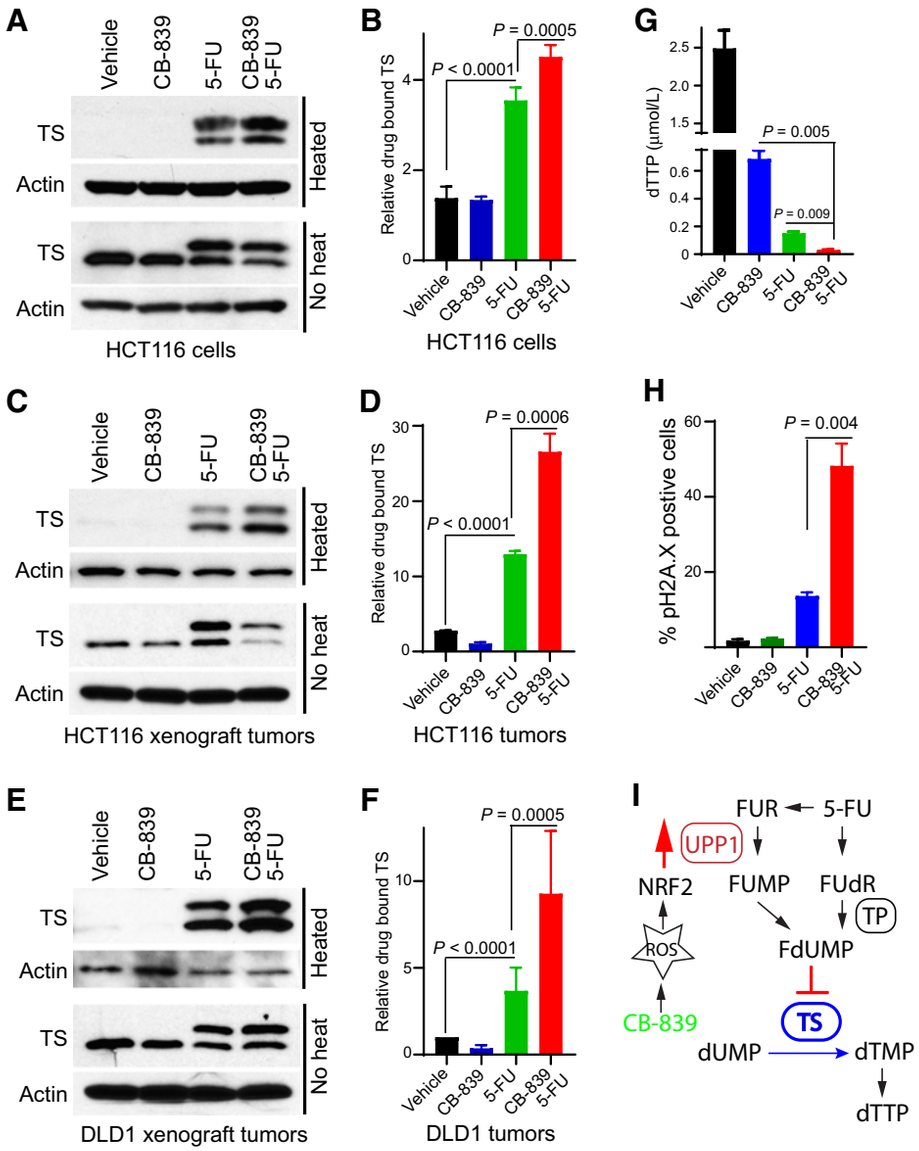

Figure 5.

CB-839 increases 5-FU toxicity through enhanced TS inhibition. **A–F,** Cellular thermal shift assay of the indicated cells or tumors treated with vehicle, CB-839, 5-FU, or the combination. Cell or tumor lysates underwent cellular thermal shift assays by either Western blot analysis (**A**, **C**, and **E**) or Alpha-ELISA (**B**, **D**, and **F**). **G,** The combination of CB-839 and 5-FU treatment depletes cellular dTTP levels. HCT116 cells were treated with the indicated drugs. Cellular dTTP amounts were measured by LC/MS-MS. The *t* test was performed for the statistical analyses. **H,** The combination of CB-839 and 5-FU treatment induces DNA damage. HCT116 cells were treated with the indicated drugs. Cells were stained with an anti-pH2A.X antibody (Supplementary Fig. S5A), and pH2A.X positive cells were counted. **I,** Schematic of the mechanism of CB-839 treatment enhancing 5-FU toxicity. FUR, fluorouridine; FUMP, fluorouridine monophosphate; FUdR, fluorodeoxyuridine; FdUMP, fluorodeoxyuridine triphosphate. The *t* test was used for statistical analyses.

Eligible patients were treated with CB-839 by mouth twice daily continuously and with capecitabine by mouth twice daily on days 1 to 14 of a 21-day treatment cycle (see study design and eligibility criteria in the materials and methods section). Dosing was based on a standard 3+3 dose escalation schedule with CB-839 ranging from 400 mg by mouth twice daily to 800 mg by mouth twice daily, as a previous phase I clinical trial shows that CB-839 as a single agent is well tolerated with a biologically active dose of 600 mg orally twice daily (43). Capecitabine dosing ranged from 750 mg/m^2 twice daily (on days 1–14) to 1,000 mg/m^2 twice daily (on days 1–14), a dose level commonly used against a variety of cancers (**Fig. 7A**; Supplementary Fig. S6A).

A total of 16 patients were enrolled in the study. Patient demographics are presented in Supplementary Table S1. Although patients with any solid tumor were permitted, 12 of 16 patients had a colorectal or appendiceal primary malignancy. The median age of participants was 68.5 years (range: 42–79) and the mean number of treatment cycles received was 5.6 (range: 1–17). Although not required for study participation, among the colorectal cancer/appendiceal patients, 7 were noted to have a *PIK3CA* mutation, 9 harbored a *KRAS* mutation, and 5 had both *PIK3CA* and *KRAS* mutations (Supplementary Table S2).

Toxicity was assessed utilizing the CTCAE version 4.0 and toxicities for patients on the study are shown in Supplementary Table S3. No DLTs were observed for any patient on the trial and the fourth and final dose level of CB-839 800 mg by mouth twice daily continuously and capecitabine 1,000 mg/m^2 orally twice daily on days 1 to 14 of a 21-day treatment cycle was recommended to be used in further phase II trials of this drug combination.

Response to therapy was assessed per RECIST 1.1 with CT imaging obtained every 9 weeks (Supplementary Fig. S6A). Of the 16 enrolled patients, 14 were evaluable for response. There were no complete responses or partial responses (Supplementary Fig. S6B). Ten and four patients had stable disease and progressive disease as their best response, respectively. Time-on-treatment (time from initiation of study treatment to coming off study) for each patient is shown in **Fig. 7A**. The median time on treatment for all patients was

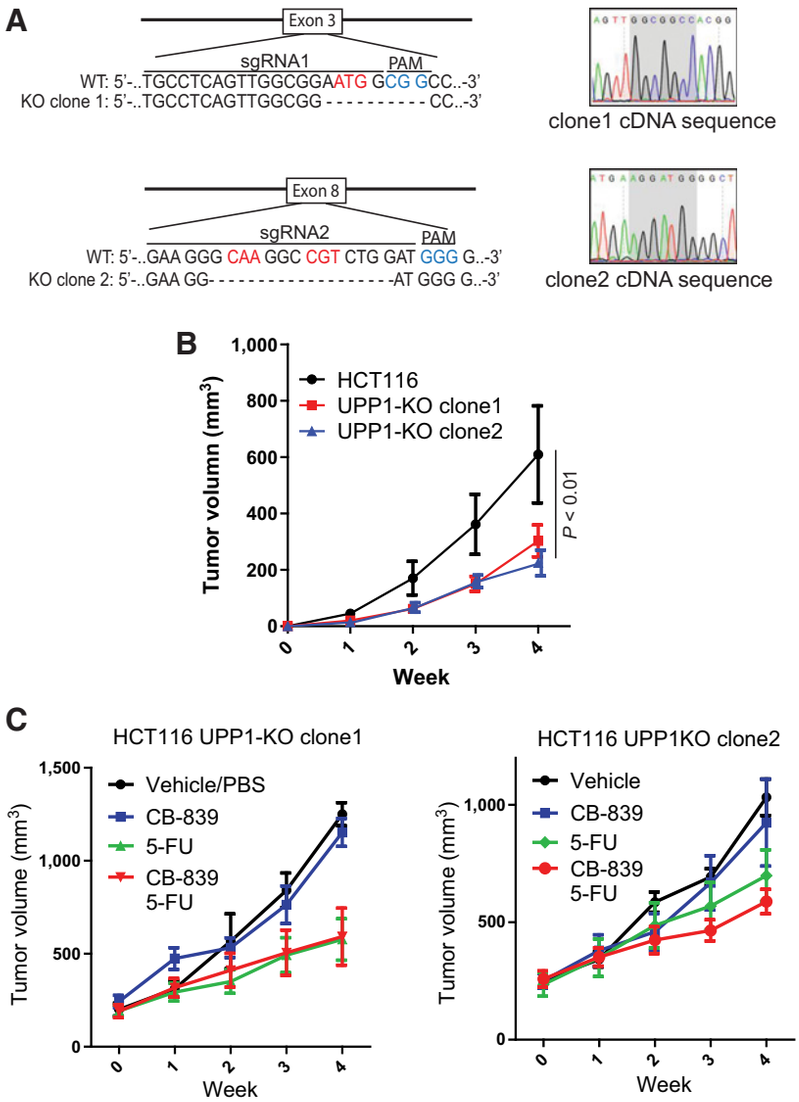

Figure 6.
UPP1 KO abrogates the interaction between CB-839 and 5-FU. **A,** Schematics of two different strategies to knockout *UPP1* with sgDNA targeting exons 3 and 8, respectively (left), and cDNA sequences of two HCT116 clones with out-of-frame deletions in the two exons are shown (right). **B,** *UPP1* knockout reduces xenograft tumor growth. HCT116 parental cells and the two UPP1 KO clones were injected subcutaneously into athymic nude mice. Tumor size was measured weekly. ANOVA was used for statistical analyses. **C,** The indicated UPP1 KO clones were injected into nude mice. When the tumors reached an average size of 200 mm^3, mice were treated with the indicated drugs.

17.9 weeks. For patients with *PIK3CA*-mutant colorectal cancer, the mean time-on-treatment was 19.9 weeks versus 16 weeks for patients with wild-type *PIK3CA* colorectal cancer. PFS among all patients was 18.75 weeks. In an exploratory Kaplan–Meier analysis (**Fig. 7B**), median PFS for patients with colorectal cancer with *PIK3CA*-mutant tumors was 24.8 (95% CI, 18.8–NA) weeks versus 16 (95% CI, 9.1–NA) weeks for patients with *PIK3CA*-WT colorectal cancer (log rank *P*-value = 0.196). However, the median PFSs of the patients on first-line fluoropyrimidine-based chemotherapy were similar between the two groups (Supplementary Fig. S6C). Note that median time-on-treatment is reduced in the *PIK3CA*-mutant group due to inclusion in the time on treatment analysis of one patient who elected to terminate the study after 4 weeks for reasons unrelated to disease progression, and who is thus censored in the analysis of PFS. Because *KRAS* mutations often co-occur with *PIK3CA* mutations, we performed Kaplan–Meier analysis according to *KRAS* mutation status. As shown in Supplementary Fig. S6D, the median PFS for the patients with colorectal cancer with *KRAS*-mutant colorectal cancer was 19 weeks versus 30 weeks for patients with *KRAS*-WT colorectal cancer (log rank *P*-value = 0.8), suggesting KRAS mutations do not sensitize colorectal cancer to the combinational drug treatment.

Discussion

Our data show that the combination of CB-839 and 5-FU induced tumor regression in three different *PIK3CA*-mutant colorectal cancer xenograft models. One-third of tumors in these models were cured. These results suggest the hypothesis that the drug combination may be an effective treatment for patients with colorectal cancer whose tumors harbor *PIK3CA* mutations. This is further supported by the results of our initial phase I trial, where an exploratory subgroup analysis of *PIK3CA*-mutant patients with colorectal cancer suggests a trend of clinical benefit as compared with *PIK3CA*-WT patients (time-on-treatment of 19.9 weeks vs. 16 weeks and exploratory PFS of 24.8 weeks vs. 16 weeks). Given that previous studies demonstrated that *PIK3CA* mutant patients with colorectal cancer have either worse survival than or no difference from *PIK3CA* WT patients with colorectal cancer after first-line treatment (5-FU-based therapy), the observed suggestive

Figure 7.

Phase I clinical trial of CB-839 plus capecitabine in humans shows the drug combination is well-tolerated. **A,** Dose escalation schedule and swimmer plot representing weeks on treatment. See Supplementary Table S3 for treatment-related adverse events. Red-filled bar, *PIK3CA*-mutant patients with colorectal cancer; black-filled bar, *PIK3CA*-WT patients with colorectal cancer; red open bar, *PIK3CA*-mutant patients with non-colorectal cancer; black open bar, *PIK3CA*-WT patients with non-colorectal cancer. **B,** PFS of *PIK3CA* WT vs. mutant patients with colorectal cancer. Kaplan–Meier curve of PFS of patients with colorectal cancer. #1, patient who came off the study due to toxicity at 16.9 weeks on treatment; this patient went onto another clinical trial and had stable disease at 21 weeks; #2, patient who went off study at 4 weeks to receive radiation therapy for a bone metastasis unrelated to disease progression and thought to be present at the time of study initiation. The patients indicated by #1 and #2 were censored at 21 and 4 weeks, respectively, due to withdrawal from the study for reasons unrelated to disease progression.

A **Dose escalation schedule**

Dose level	CB-839 (mg) orally twice daily for 21 days	Capecitabine (mg/m^2) orally twice daily for 14/21 days
1	400	750
2	600	750
3	600	1,000
4	800	1,000

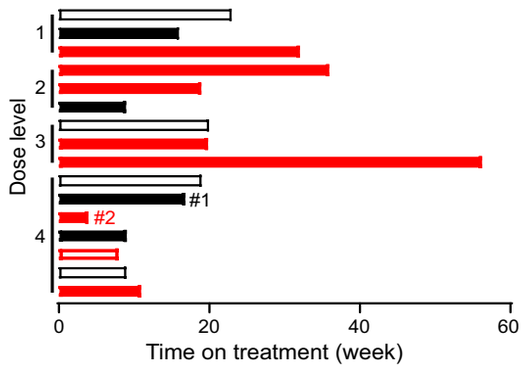

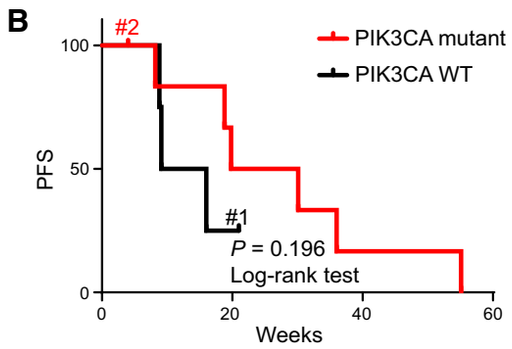

clinical benefit of *PIK3CA*-mutant patients with colorectal cancer is unlikely to be due to differential response to 5-FU between *PIK3CA* mutant and WT patients (44, 45). A limitation of this phase 1 study is the small size of the cohort that assessed only 12 patients with colorectal/appendiceal cancer in total and treated most patients at lower doses of the capecitabine/CB-839 combination. However, the promising nature of the results warrant our now ongoing phase II trial to more fully evaluate the activity of this approach, specifically in *PIK3CA*-mutant patients with colorectal cancer treated at maximal drug levels (NCT02861300).

Mechanistically, CB-839 treatment upregulates the expression of UPP1, an enzyme facilitating conversion of 5-FU to active compound FdUMP, which in turn enhances the tumor inhibitory effect of 5-FU. We provide here three lines of evidence to support this notion: (i) CB-839 enhances the binding of FdUMP to TS in both culture cells and in xenograft tumors (**Fig. 5**); (ii) knockout of UPP1 abrogates the tumor inhibitory effect of combined CB-839 and 5-FU (**Fig. 6**); and (iii) the combination of CB-839 and 5-FU depletes cellular dTTP, a major product of TS (**Fig. 5**). It is worth noting that knockout of UPP1 slows down xenograft tumor growth of HCT116 cells, which may be due to the role of UPP1 in the salvage nucleotide synthesis pathway (41). Moreover, knockout of *UPP1* does not have a significant impact on 5-FU treatment (**Fig. 6C**), which may be because 5-FU can still be converted to FdUPM by thymidine phosphorylase (**Fig. 5I**). Interestingly, *UPP1* knockout also abrogates the effect of CB-839 (**Fig. 6C**). We postulate that knockout of *UPP1* may activate a pathway(s) that compensates the impact of glutaminase inhibition. Nonetheless, our data are consistent with previous studies showing that UPP1 knockout mouse embryonic stem cells are resistant to 5-FU (30), whereas overexpression of UPP1 enhances the cytotoxicity of 5-FU (46). Our studies reveal that CB-839 treatment increases ROS levels, which lead to nuclear translocation of Nrf2 and increased transcription of UPP1 (**Fig. 4**). Here we focused the studies on the tumor-intrinsic effect of the combination of CB-839 and 5-FU. However, it is possible that the drug combination may also impact tumor microenvironments, especially the immune cells, as well, which warrants further investigation.

Finally, our study provides further evidence supporting the notion that *PIK3CA*-mutant colorectal cancers are more dependent on glutamine. Our previous isotope-tracing studies in cultured cells and xenograft tumors showed that *PIK3CA*-mutant colorectal cancers utilized more glutamine to replenish the TCA cycle than the isogenic *PIKCA* WT colorectal cancers (3, 19). However, tumors established from the isogenic *PIK3CA*-mutant and WT HCT116 cell lines use

similar amounts of glucose to fuel the TCA cycle (3). We previously reported that *PIK3CA* mutations render colorectal cancers dependent on glutamine through the upregulation of GPT2 (19). We further demonstrated that aminooxyacetate, which blocks the second step of glutamine metabolism, suppresses xenograft tumor growth of *PIK3CA*-mutant, but not WT, colorectal cancer (19). We show here that blocking the first step of glutamine metabolism by CB-839 also preferentially inhibits xenograft tumor growth of *PIK3CA*-mutant colorectal cancers. This is again consistent with what we observed in patients during our clinical trial. Interestingly, loss of PTEN, the enzyme that catalyzes the opposite reaction of *PIK3CA*/p110α, also renders breast cancers dependent on glutamine (47). These observations indicate that the PI3K pathway plays a critical role in modulating glutamine metabolism in certain cancer types and support proceeding to phase II human trials for further evaluation of glutamine metabolism as a therapeutic target for human *PIK3CA*-mutant cancers.

Disclosure of Potential Conflicts of Interest

J.S. Barnholtz-Sloan reports grants from NIH during the conduct of the study. S. Vinayak reports other funding from Oncosec (direct funding to institution for clinical trial), Pfizer (direct funding to institution for clinical trial), and Seattle Genetics (direct funding to institution for clinical trial) outside the submitted work. N.J. Meropol reports grants from NIH during the conduct of the study, other compensation from Flatiron Health (employment, equity interest) and Roche (equity ownership) outside the submitted work, and a patent for US Patent Office 20020031515 issued (Methods of therapy for cancers characterized by over expression of the HER2 receptor protein; expires May 14, 2021). J.R. Eads reports grants from NIH and Stand Up 2 Cancer during the conduct of the study; personal fees from Pfizer (honoraria for giving a talk), Ipsen (advisory board), Lexicon (consulting), Novartis (advisory board), Advanced Accelerator Applications (advisory board), grants from Incyte (research funding), and personal fees from Bristol Meyers Squibb (husband is an employee) outside the submitted work. Z. Wang reports grants from NCI and SU2C during the conduct of the study and a patent for 10221459 issued. No potential conflicts of interest were disclosed by the other authors.

Authors' Contributions

Y. Zhao: Conceptualization, data curation, investigation, writing-original draft, writing-review and editing. **X. Feng:** Data curation, investigation. **Y. Chen:** Data curation, investigation, methodology. **J.E. Selfridge:** Data curation. **S. Gorityala:** Investigation. **Z. Du:** Investigation. **J.M. Wang:** Data curation, formal analysis. **Y. Hao:** Investigation. **G. Cioffi:** Formal analysis. **R.A. Conlon:** Resources, writing-review and editing. **J.S. Barnholtz-Sloan:** Formal analysis. **J. Saltzman:** Recruited patients. **S.S. Krishnamurthi:** Recruited patients. **S. Vinayak:** Recruited patients. **M. Veigl:** Data curation, investigation. **Y. Xu:** Data curation, investigation. **D.L. Bajor:** Recruited patients. **S.D. Markowitz:** Conceptualization, resources. **N.J. Meropol:** Conceptualization, writing-review and editing, recruited patients. **J.R. Eads:** Conceptualization, data curation, supervision, writing-original draft, project administration, writing-review and editing, recruited patients. **Z. Wang:** Conceptualization, formal analysis, supervision, funding acquisition, writing-original draft, project administration, writing-review and editing.

Acknowledgments

The authors would like to thank Drs. Lewis Cantley, John Pink, and Robert B. Diasio for suggestions and discussions. This work was supported by NIH grants R01CA196643, UH2CA223670, P50CA150964, and P30 CA043703. This work was also supported by a Stand Up to Cancer Colorectal Cancer Dream Team Translational Research Grant (Grant No. SU2C-AACR-DT22-17). Stand Up to Cancer is a division of the Entertainment Industry Foundation. Research grants are administered by the American Association for Cancer Research, a scientific partner of SU2C. This research was further supported by the Gene Expression and Genotyping Facility of the Case Comprehensive Cancer Center (P30 CA043703). Calithera Biosciences provided CB-839 for preclinical and clinical studies as well as financial support for patient enrollment.

The costs of publication of this article were defrayed in part by the payment of page charges. This article must therefore be hereby marked *advertisement* in accordance with 18 U.S.C. Section 1734 solely to indicate this fact.

Received February 21, 2020; revised July 6, 2020; accepted September 3, 2020; published first September 9, 2020.

References

1. Zhang J, Pavlova NN, Thompson CB. Cancer cell metabolism: the essential role of the nonessential amino acid, glutamine. EMBO J 2017;36:1302–15.
2. Altman BJ, Stine ZE, Dang CV. From Krebs to clinic: glutamine metabolism to cancer therapy. Nat Rev Cancer 2016;16:619–34.
3. Zhao Y, Zhao X, Chen V, Feng Y, Wang L, Croniger C, et al. Colorectal cancers utilize glutamine as an anaplerotic substrate of the TCA cycle in vivo. Sci Rep 2019;9:19180.
4. Gross MI, Demo SD, Dennison JB, Chen L, Chernov-Rogan T, Goyal B, et al. Antitumor activity of the glutaminase inhibitor CB-839 in triple-negative breast cancer. Mol Cancer Ther 2014;13:890–901.
5. Elgogary A, Xu Q, Poore B, Alt J, Zimmermann SC, Zhao L, et al. Combination therapy with BPTES nanoparticles and metformin targets the metabolic heterogeneity of pancreatic cancer. Proc Natl Acad Sci U S A 2016;113:E5328–36.
6. Meric-Bernstam F, Tannir NM, Mier JW, DeMichele A, Telli ML, Fan AC, et al. Phase 1 study of CB-839, a small molecule inhibitor of glutaminase (GLS), alone and in combination with everolimus (E) in patients (pts) with renal cell cancer (RCC). J Clin Oncol 2016;34:4568.
7. Gregory MA, Nemkov T, Reisz JA, Zaberezhnyy V, Hansen KC, D'Alessandro A, et al. Glutaminase inhibition improves FLT3 inhibitor therapy for acute myeloid leukemia. Exp Hematol 2018;58:52–8.
8. Davidson SM, Papagiannakopoulos T, Olenchock BA, Heyman JE, Keibler MA, Luengo A, et al. Environment impacts the metabolic dependencies of ras-driven non-small cell lung cancer. Cell Metab 2016;23:517–28.
9. Romero R, Sayin VI, Davidson SM, Bauer MR, Singh SX, LeBoeuf SE, et al. Keap1 loss promotes Kras-driven lung cancer and results in dependence on glutaminolysis. Nat Med 2017;23:1362–8.
10. Momcilovic M, Bailey ST, Lee JT, Fishbein MC, Braas D, Go J, et al. The GSK3 signaling axis regulates adaptive glutamine metabolism in lung squamous cell carcinoma. Cancer Cell 2018;33:905–21.
11. Momcilovic M, Bailey ST, Lee JT, Fishbein MC, Magyar C, Braas D, et al. Targeted inhibition of EGFR and glutaminase induces metabolic crisis in EGFR mutant lung cancer. Cell Rep 2017;18:601–10.
12. Matre P, Velez J, Jacamo R, Qi Y, Su X, Cai T, et al. Inhibiting glutaminase in acute myeloid leukemia: metabolic dependency of selected AML subtypes. Oncotarget 2016;7:79722–35.
13. Xu X, Meng Y, Li L, Xu P, Wang J, Li Z, et al. Overview of the development of glutaminase inhibitors: achievements and future directions. J Med Chem 2019;62:1096–115.
14. Fruman DA, Chiu H, Hopkins BD, Bagrodia S, Cantley LC, Abraham RT. The PI3K pathway in human disease. Cell 2017;170:605–35.
15. Liu P, Cheng H, Roberts TM, Zhao JJ. Targeting the phosphoinositide 3-kinase pathway in cancer. Nat Rev Drug Discov 2009;8:627–44.
16. Lawrence MS, Stojanov P, Mermel CH, Robinson JT, Garraway LA, Golub TR, et al. Discovery and saturation analysis of cancer genes across 21 tumour types. Nature 2014;505:495–501.
17. Samuels Y, Wang Z, Bardelli A, Silliman N, Ptak J, Szabo S, et al. High frequency of mutations of the PIK3CA gene in human cancers. Science 2004;304:554.
18. Thorpe LM, Yuzugullu H, Zhao JJ. PI3K in cancer: divergent roles of isoforms, modes of activation and therapeutic targeting. Nat Rev Cancer 2015;15:7–24.
19. Hao Y, Samuels Y, Li Q, Krokowski D, Guan BJ, Wang C, et al. Oncogenic PIK3CA mutations reprogram glutamine metabolism in colorectal cancer. Nat Commun 2016;7:11971.
20. Feng X, Hao Y, Wang Z. Targeting glutamine metabolism in PIK3CA mutant colorectal cancers. Genes Dis 2016;3:241–3.
21. Hao Y, Wang C, Cao B, Hirsch BM, Song J, Markowitz SD, et al. Gain of interaction with IRS1 by p110alpha-helical domain mutants is crucial for their oncogenic functions. Cancer Cell 2013;23:583–93.

22. Zhao Y, Zhang X, Guda K, Lawrence E, Sun Q, Watanabe T, et al. Identification and functional characterization of paxillin as a target of protein tyrosine phosphatase receptor T. Proc Natl Acad Sci U S A 2010;107:2592–7.
23. Du Z, Song J, Wang Y, Zhao Y, Guda K, Yang S, et al. DNMT1 stability is regulated by proteins coordinating deubiquitination and acetylation-driven ubiquitination. Sci Signal 2010;3:ra80.
24. Zhao Y, Scott A, Zhang P, Hao Y, Feng X, Somasundaram S, et al. Regulation of paxillin-p130-PI3K-AKT signaling axis by Src and PTPRT impacts colon tumorigenesis. Oncotarget 2016;8:48782.
25. Zhang X, Guo C, Chen Y, Shulha HP, Schnetz MP, LaFramboise T, et al. Epitope tagging of endogenous proteins for genome-wide ChIP-chip studies. Nat Methods 2008;5:163–5.
26. Axelsson H, Almqvist H, Seashore-Ludlow B, Lundback T. Screening for target engagement using the cellular thermal shift assay - CETSA. In: Sittampalam GS, Grossman A, Brimacombe K, Arkin M, Auld D, Austin CP, et al., editors. Assay guidance manual. Bethesda, MD: Eli Lilly & Company and the National Center for Advancing Translational Sciences, 2004; p. 649–73.
27. Zhang X, Guo A, Yu J, Possemato A, Chen Y, Zheng W, et al. Identification of STAT3 as a substrate of receptor protein tyrosine phosphatase T. Proc Natl Acad Sci 2007;104:4060–4.
28. Chen Y, Zhao Y, Bajor DL, Wang Z, Selfridge JE. A facile and sensitive method of quantifying glutaminase binding to its inhibitor CB-839 in tissues. Journal of Genetics and Genomics 2020 Jun 16 [Epub ahead of print].
29. Cao D, Pizzorno G. Uridine phosophorylase: an important enzyme in pyrimidine metabolism and fluoropyrimidine activation. Drugs of today 2004;40:431–43.
30. Cao D, Russell RL, Zhang D, Leffert JJ, Pizzorno G. Uridine phosphorylase (-/-) murine embryonic stem cells clarify the key role of this enzyme in the regulation of the pyrimidine salvage pathway and in the activation of fluoropyrimidines. Cancer Res 2002;62:2313–7.
31. Remy S, Verstraelen S, Van Den Heuvel R, Nelissen I, Lambrechts N, Hooyberghs J, et al. Gene expressions changes in bronchial epithelial cells: markers for respiratory sensitizers and exploration of the NRF2 pathway. Toxicol in Vitro 2014;28:209–17.
32. Dodson M, Redmann M, Rajasekaran NS, Darley-Usmar V, Zhang J. KEAP1-NRF2 signalling and autophagy in protection against oxidative and reductive proteotoxicity. Biochem J 2015;469:347–55.
33. Son J, Lyssiotis CA, Ying H, Wang X, Hua S, Ligorio M, et al. Glutamine supports pancreatic cancer growth through a KRAS-regulated metabolic pathway. Nature 2013;496:101–5.
34. Gwinn DM, Lee AG, Briones-Martin-Del-Campo M, Conn CS, Simpson DR, Scott AI, et al. Oncogenic KRAS regulates amino acid homeostasis and asparagine biosynthesis via ATF4 and alters sensitivity to L-asparaginase. Cancer Cell 2018;33:91–107.
35. Shin CS, Mishra P, Watrous JD, Carelli V, D'Aurelio M, Jain M, et al. The glutamate/cystine xCT antiporter antagonizes glutamine metabolism and reduces nutrient flexibility. Nat Commun 2017;8:15074.
36. Muir A, Danai LV, Gui DY, Waingarten CY, Lewis CA, Vander Heiden MG. Environmental cystine drives glutamine anaplerosis and sensitizes cancer cells to glutaminase inhibition. Elife 2017;6:e27713.
37. Maher JM, Aleksunes LM, Dieter MZ, Tanaka Y, Peters JM, Manautou JE, et al. Nrf2- and PPAR alpha-mediated regulation of hepatic Mrp transporters after exposure to perfluorooctanoic acid and perfluorodecanoic acid. Toxicol Sci 2008;106:319–28.
38. Pratt S, Shepard RL, Kandasamy RA, Johnston PA, Perry W, 3rd, Dantzig AH. The multidrug resistance protein 5 (ABCC5) confers resistance to 5-fluorouracil and transports its monophosphorylated metabolites. Mol Cancer Ther 2005;4:855–63.
39. Oguri T, Bessho Y, Achiwa H, Ozasa H, Maeno K, Maeda H, et al. MRP8/ABCC11 directly confers resistance to 5-fluorouracil. Mol Cancer Ther 2007;6:122–7.
40. Martinez Molina D, Jafari R, Ignatushchenko M, Seki T, Larsson EA, Dan C, et al. Monitoring drug target engagement in cells and tissues using the cellular thermal shift assay. Science 2013;341:84–7.
41. Longley DB, Harkin DP, Johnston PG. 5-fluorouracil: mechanisms of action and clinical strategies. Nat Rev Cancer 2003;3:330–8.
42. Pai CC, Kearsey SE. A critical balance: dNTPs and the maintenance of genome stability. Genes 2017;8:57.
43. Harding JJ, Telli ML, Munster PN, Le MH, Molineaux C, Bennett MK, et al. Safety and tolerability of increasing doses of CB-839, a first-in-class, orally administered small molecule inhibitor of glutaminase, in solid tumors. 2015;33:2512.
44. Wang Q, Shi YL, Zhou K, Wang LL, Yan ZX, Liu YL, et al. PIK3CA mutations confer resistance to first-line chemotherapy in colorectal cancer. Cell Death Dis 2018;9:739.
45. Ogino S, Liao X, Imamura Y, Yamauchi M, McCleary NJ, Ng K, et al. Predictive and prognostic analysis of PIK3CA mutation in stage III colon cancer intergroup trial. J Natl Cancer Inst 2013;105:1789–98.
46. Im YS, Shin HK, Kim HR, Jeong SH, Kim SR, Kim YM, et al. Enhanced cytotoxicity of 5-FU by bFGF through up-regulation of uridine phosphorylase 1. Mol Cells 2009;28:119–24.
47. Mathur D, Stratikopoulos E, Ozturk S, Steinbach N, Pegno S, Schoenfeld S, et al. PTEN Regulates glutamine flux to pyrimidine synthesis and sensitivity to dihydroorotate dehydrogenase inhibition. Cancer Discov 2017;7:380–90.